

# Experimental and Numerical Investigation Of Controlled Rotomolded Axial Fan By Internal Air Injection At Gap Clearance

Ayoub BOUANIK<sup>1,2</sup>, Abderrahim LARABI<sup>2</sup>, Tarik AZZAM<sup>2</sup>, Mahmoud MEKADEM<sup>2</sup>, Farid BAKIR<sup>3</sup>

<sup>1</sup>Laboratoire de Recherche Energétique, Ecoulements et Transferts/Academie Militaire de Chercell  
BP 48 Chercell Terre 42067, Tipaza, Algeria

[d\\_bouanik.ayoub@emp.mdn.dz](mailto:d_bouanik.ayoub@emp.mdn.dz); [abderrahim.larabi@emp.mdn.dz](mailto:abderrahim.larabi@emp.mdn.dz); [tarik.azzam@emp.mdn.dz](mailto:tarik.azzam@emp.mdn.dz);  
[mahmoud.mekadem@emp.mdn.dz](mailto:mahmoud.mekadem@emp.mdn.dz), [Farid.BAKIR@ensam.eu](mailto:Farid.BAKIR@ensam.eu).

<sup>2</sup>Laboratoire Mécanique des Fluides/Ecole Militaire Polytechnique  
BP 17 Bordj El Bahri 16214, Algiers, Algeria

<sup>3</sup>Arts et Métiers Institute of Technology, CNAM, LIFSE, HESAM University, F-75013 Paris, France.

**Abstract** - In the present era, axial fans play a pivotal role in crucial sectors of both industry and research. As a result, significant attention has been directed towards enhancing their aerodynamic performances. The ongoing inquiry is centered around elevating the aerodynamic efficiencies of a fan produced through rotational molding techniques. First is adopting an active control by injecting a compressed air through 16 holes placed at the fan's hollow shroud ring of a dimension of 4 mm, by leveraging a benefit that involves in exploiting the hollow nature of the fan with the centrifugal effect. In the other hand, the fan's axial position with respect to the casing was investigated to know its influence on aerodynamics performances. The numerical investigation employing the K- $\omega$  SST turbulence model allows a detailed characterization of the flow modification around the fan. Results show that the swirling zone that forms around the shroud ring in investigated axial positions as a result of the interaction of the main and leakage flows with casing walls, has a significant impact on the change of the flow topology. In comparison to the baseline case, the aerodynamic performances are improved as the leakage flow and the swirling zone are both reduced. This improvement is translated into a gain of approximately 53% in aerodynamic power and a leakage flow reduction of about 80%.

**Keywords:** Axial fan, leakage flow, Active control, hollow blades, holes.

## 1. Introduction

In this study, an active control technique is applied to a new generation of axial fans obtained by the rotomolding process, these axial fans were known for their advantages of lightness and hollow interior part (blades, hub, and shroud ring) which can be used as a flow channel. The overall aerodynamic parameters were previously studied in the "Laboratoire d' Ingénierie des Fluides et des Systèmes Energétiques" (LIFSE), specifically the thickness effect reported by Sarraf et al. [1] and the blades sweeping investigated by Huraut [2].

The operation of the fan is the seat of several flow-destructive phenomena, which harm both aerodynamic and acoustic performances around the fan, as represented by Squire And Winter [3], independently from the main flow, especially the tip leakage flow between the shroud ring and the casing which results from the pressure difference between the downstream and the upstream area close to the shroud ring walls. Furthermore, this resulting secondary flow was discussed through a numerical and experimental analysis conducted by Boudet et al. [4], where it was thought to be the main source of noise emission because of the Tip Leakage Vortex (TLV) generated during axial fans functioning. Furthermore, Zhu et al. [5] have reported that the TLV are deeply influenced by the tip gap size, leading to the conclusion that as the tip clearance decrease, the more sound emission is reduced. For that the choice of the clearance gap is considered as crucial step. This tip clearance has also been the subject of the work of You et al. [6] who numerically showed that the tip gap reduction has a favorable influence on the reduction of vorticity and Turbulent Kinetic Energy, sources of the TLV. To put it more properly, in order to comprehend this sound emission, Canepa et al. [7] have experimentally employed advanced characterization technics such as PIV and LDV to detail the complex flow in the tip gap region into periodic phenomena and non-periodic ones, the interaction between them cause the sound emission.

To remedy the negative effect related to tip leakage flow, several strategies of control are suitable for this sort of flow in turbomachinery, like passive or active control as two strategies that may enhance the overall performance of these kind of fans. In this regard, Azzam et al. [8] experimentally proceeded to reduce the leakage flow for the same rotomolded fan used in the present study, which lead to a gain of 53% of aeraulic power, by injecting air into the clearance gap zone through 16 and 32 holes in the shroud ring circumference. For better understanding of the behavior of this rotomolded fan with its hollow nature and the contribution of the air injection on fan performances, a detailed numerical investigation was carried out by Pereira et al. [9] which is considered as continuity of works discussed in [8]. By analyzing entropy contours over the fan, the significant energy dissipations was mainly caused by the tip leakage flow. Always in the context of the flow control in turbomachinery with hollow parts, it was found in Eberlink et al. [10] investigations, who proceeded to a passive flow injection by recovering a portion of the main flow and used it to blow air through the periphery of an axial fan and also to the suction side of an airfoil.

According to the literature, a number of flow control techniques that are either actively or passively used in turbomachinery for flow control and performance improvement, are probably applicable to this new generation of fans, particularly when operating under the same conditions, examples include ducted or unducted fans that operate in a casing, working in an enclosed environment causing a blockage effect. In this perspective, Park et al. [11] were adopted a passive control strategy, where fences were added to the casing in the passage region of the blade's tip to reduce the tip leakage vortices. Moreover, Wasilczuk et al. [12] were introduced slots to the shroud sealing for a turbine rotor and use it as a passive flow control (named air curtain), which results from it an important velocity jet through the clearance gap.

This study is focused on examining the contribution of an active control by air injection through 16 holes placed on the hollow shroud ring on performance improvement, by taking into account the axial position of the fan within the casing. The control strategy used in this study led to significant improvements in aerodynamic performances which differs from one axial position to another.

## 2. Studied fan

The present work is aiming to enhance the aerodynamic behavior of an axial rotomolded fan, which is considered as new generation, designed for engine cooling fans. Also known for their advantages of lightness due to the hollow nature of its blades and shroud ring as a result of the rotomolded process figure 1. The adopted shrouded fan has 6 blades of a 179 mm internal radius, a 195 mm of overall diameter (including the shroud ring), and a hub of 65.5 mm diameter. The use of this fan for engine cooling require operating inside a casing that needs clearance gap for any potential vibration or shaft eccentricity (4 mm of clearance gap in this study). The hollow nature of the fan was used as flow channels for an actively controlled cases by air injection.



Fig. 1: Fan with hallow blades and shroud ring [8].

## 3. Study details

The control strategy involves blowing air through 16 injection holes that are properly positioned and oriented. Two fan rotation speeds of 1000 rpm and 2000 rpm were considered for both baseline and controlled cases. In case of flow control, two injection rates of  $\xi=0.4$  and  $\xi=0.8$  are chosen, which correspond to the ratio of the injected flow rate to the maximum

one of about  $q_{max}=1000$  l/min, as shown in Eq. (1) below. to check the studied fan characteristics over a wide range of flow coefficient, several diaphragm diameters are tested, namely **238, 267, 300, 336 and 375** mm.

$$\xi = \frac{q_{inj}}{q_{max}} \quad (1)$$

### 3.1. Experimental setup

Experimental trials are carried out using a test bench presented in figure 2 constructed in accordance with the ISO 5801 standard [13] in LIFSE laboratory at Ecole Nationale Supérieure d'Arts et Métiers, Paris, French.

The hollow part of the fan is powered by a compressor with a maximum flow rate of 1000 l/min, where the flow rate is calculated using a flowmeter. A driver system ensures both the transmission of rotational movement to the fan as well as regulating air injection into the hollow components of the fan. The transmission of the rotation speed from the motor to the drive system is assured by a pulley-belt system. The drive control system was equipped with a torque meter for a better evaluation of the fan flow resistance. The system came with a frequency converter for the optimal control of the rotation speed (measured using a tachymeter).

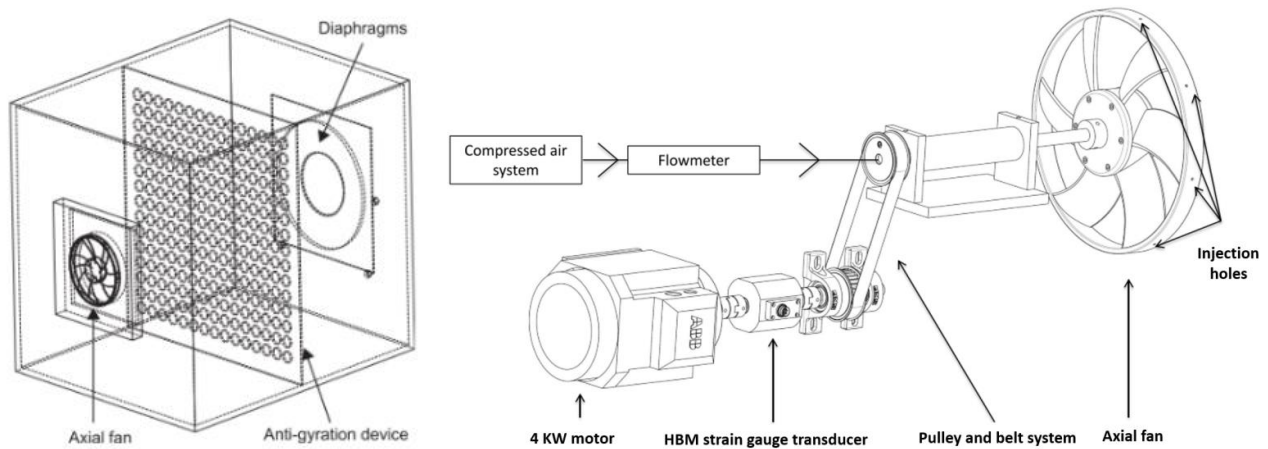


**Fig. 2 :** Test bench ISO 5801 [13] dimension  $1.3m \times 1.3m \times 1.8m$  (Left) and drive control system (right) [8].

### 3.2. Numerical setup

Usually, fans give rise to several phenomena related to the interaction of complex flows, being unsteady and three-dimensional in nature. To well explain these phenomena, steady RANS simulations using ANSYS Fluent were performed in this work, coupled with the  $k-\omega$  SST turbulence model, which is extensively used in turbomachinery.

The computational domain adopted during this investigation consists of the ISO5801 test bench, the fan geometry, and both the inlet and outlet fluid volume as shown in figure 3. The generated mesh consists of polyhedral cells, with special attention is made to refine the zones of interest especially blades, shroud ring, hub, clearance gap, and also the suction zone inside the test bench, to get approximately a value of  $y^+ = 1$  (figure 3).

For all computations, the pressure-based solver was used with the SIMPLE coupling algorithm for velocity and pressure treatments. It is significant to highlight that the MRF (Moving Reference Frame) was used for fan rotation modelling. For the discretization schemes, the MUSCL third-order schemes for momentum and the second-order for the remaining equations. For turbulence intensity, it was chosen to be about a value of 1%, and the value of 1 was chosen for the turbulence viscosity ratio.

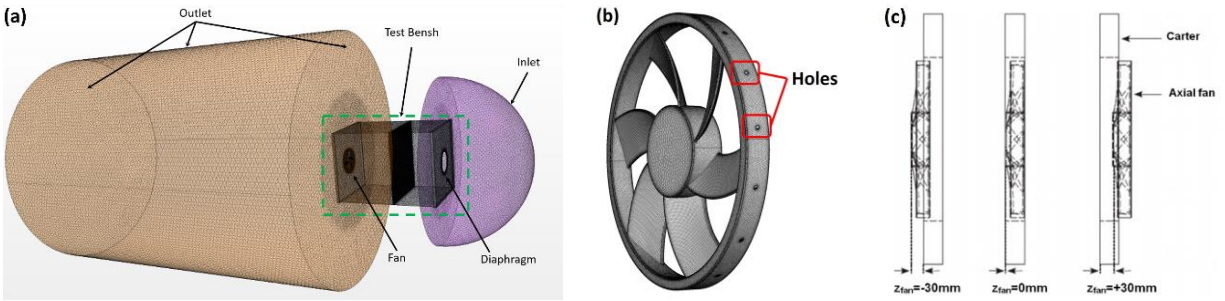


**Fig. 3 :** (a) 3D numerical whole domain (b) Hollow fan hexahedral mesh (c) Schematic of the adopted axial position of the fan [8].

## 4. Results

### 4.1. Axial position Influence

#### 4.1.1 Fan characteristics

The leakage flow is influenced by the fan's axial position within the casing as well as its rotating speed and flow rate. When assembling, this geometrical characteristic should be taken into account. For that, three positions (-30 mm, 0 mm, 30 mm) were tested for baseline and 16 holes air injection-controlled cases to examine its impact (see figure 3c).

It was noticed that for 1000 rpm fan speed, its characteristics are significantly improved at the location  $z_{fan} = 0$  mm, especially toward the high flows rate. Figure 4 depicts the overall performances for the both rotation speed 1000 rpm and 2000 rpm. Thus, improvements shown at 1000 rpm progressively decrease with increasing rotational speed, especially at low flow coefficients. Additionally, it is highlighted that the control becomes unfavorable to the aerodynamic performances for low flow rates (diaphragm diameters = 238 mm, 267 mm, and 300 mm) for the  $z_{fan} = +30$  mm position. Consequently, the fan was positioned at  $z_{fan} = 0$  mm which is adopted for the upcoming investigations (Section 4.2 and 4.3).

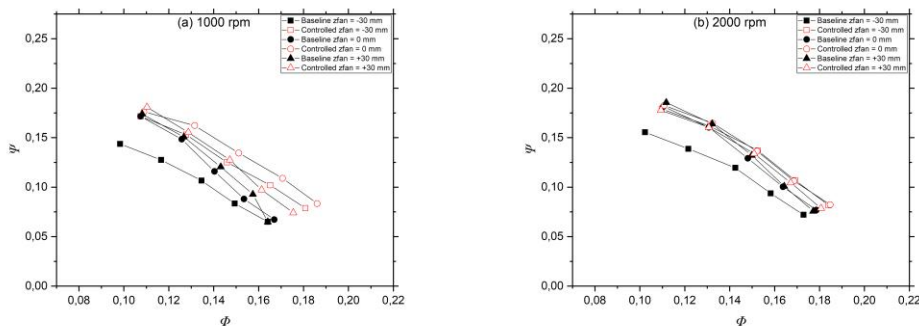


**Fig. 4:** Influence of the axial position on the fan characteristics.

#### 4.1.2 Flow structure

For a better understanding of the effect of the fan's axial location relative to the casing on the flow topology and fan performance in both baseline and controlled cases, we focused on the lower and higher flow coefficients corresponding to the 238 mm and 375 mm diaphragm diameters, respectively, for the rotation speed 1000 rpm when the maximum improvement in aerodynamics performances.

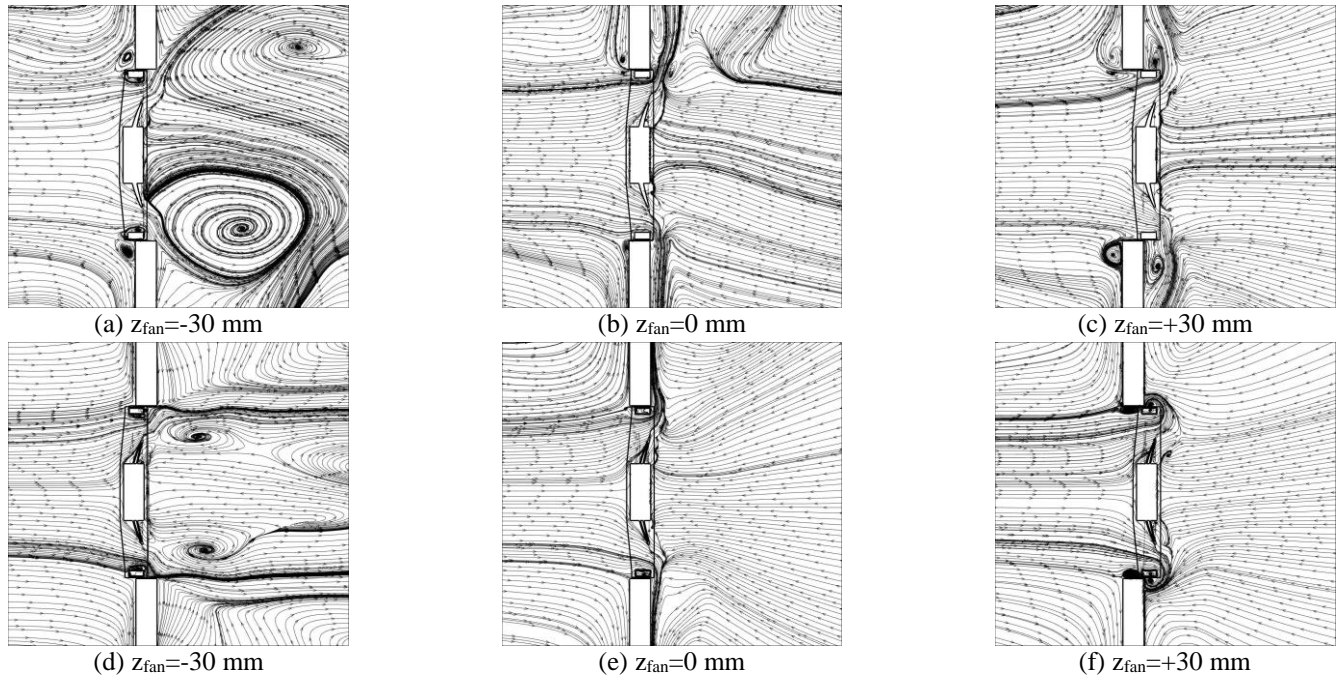


**Fig. 5:** Flow structure for the diaphragm diameter 238, rotating speed 1000 rpm.  
 (a), (b) and (c): Baseline cases. (d), (e) and (f): 16 holes-controlled cases  $\xi = 0.8$ .  
 (Flow from left to right).

For the diaphragm diameter 238 in the fan positions  $z_{fan} = 0$  mm and  $z_{fan} = +30$  mm figure 5 (b) and (c) and confirmed by the Q criterion analyses in figure 6 (b) and (c), it can be observed that the flow is directed towards the radial direction when the fan operates at a low flow rate under the effect of blades sweeping, which generates a recirculation zone close to the shroud ring and the casing upstream and downstream of the fan, In the controlled cases figure 5 (e) and (f) results show that these recirculation zones were reduced and attached to the fan's shroud ring. At the fan position  $z_{fan} = -30$  mm figure 5 (a) and figure 6 (a), the presence of the casing in the radial way of the flow involves the enlargement of this recirculation zone in the downstream direction in the baseline case, and the approach of the recirculation zone upstream of the fan to the shroud ring. In controlled cases, it is observed that the injection jet flow involves a redirection of the main flow from the radial to the axial direction near the gap radial position as air is absorbed from the far field in the other radial position zones, with the birth of two recirculation zone opposed to blades figure 5 (d) and figure 6 (d).

For the diaphragm diameter of 375 mm figure 7 and figure 8, the flow is characterized by high inertial forces, which drive the flow downstream of the fan in the axial direction over all fan's axial positions. It is observed also in the position  $z_{fan} = +30$  mm, the formation of a recirculation zone upstream of the fan and inside the casing region, this recirculation zone is smaller in the other positions. In the controlled case in the same position, a big recirculation zone was also formed near the shroud ring, which leads to the deviation of the main flow to the radial direction, this zone is smaller in the case of a diaphragm diameter of 238 mm likely because of the low inertial force compared to the case of the 375 mm.



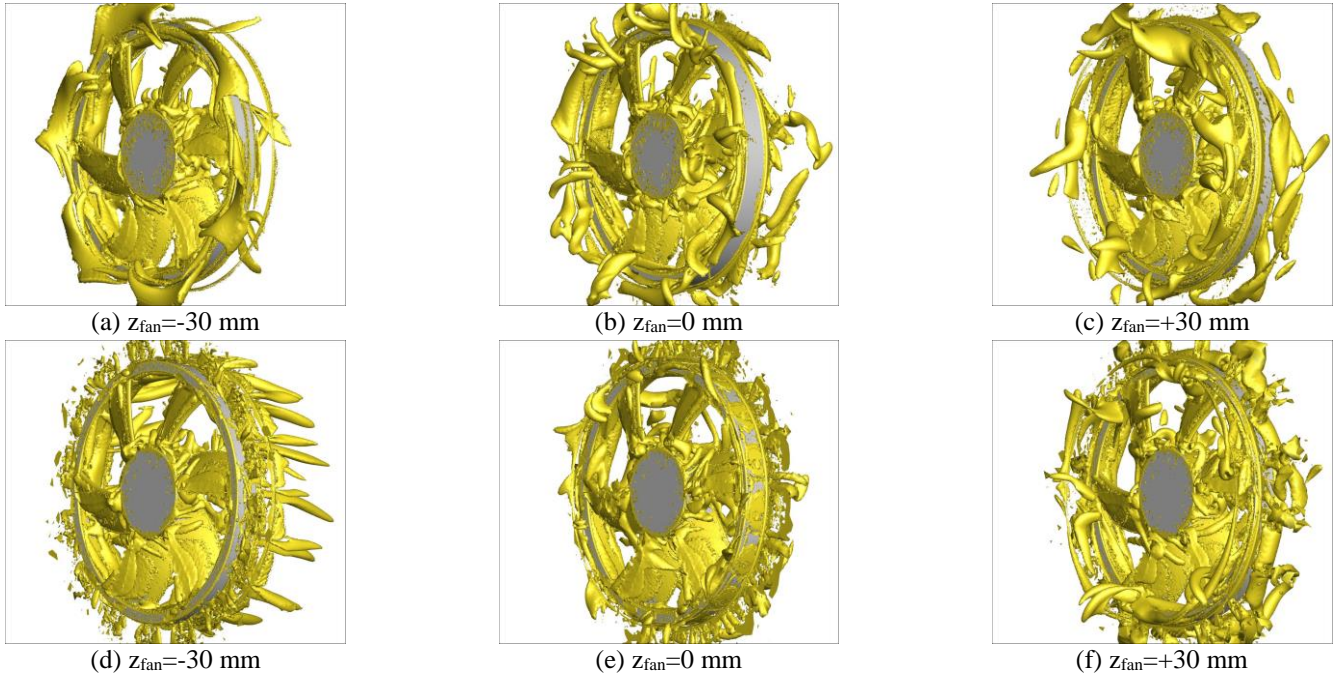


**Fig. 6:** Vorticity analyses using Q criterion for the diaphragm diameter 238 mm, rotating speed 1000 rpm.  
 (a), (b) and (c) : Baseline cases. (d), (e) and (f): 16 holes-controlled cases  $\xi = 0.8$ .  
**(Flow from left to right).**

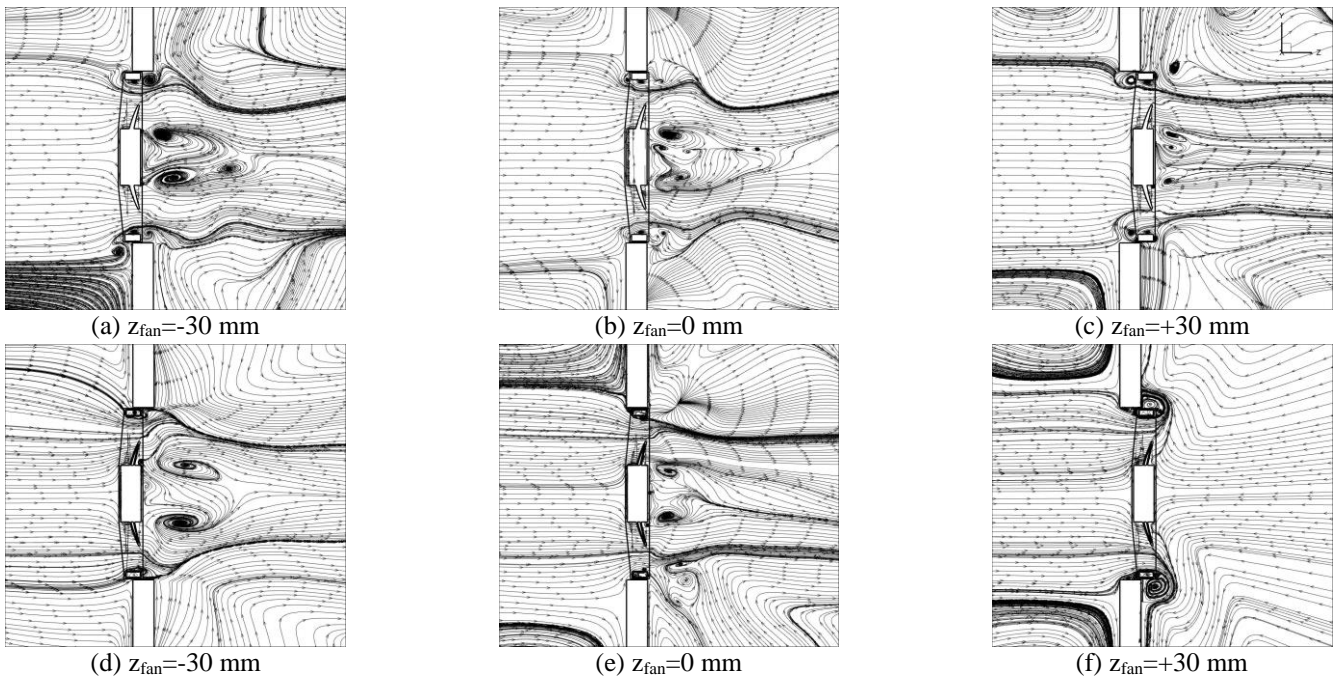


**Fig. 7:** Flow structure for the diaphragm diameter 375, rotating speed 1000 rpm.  
 (a), (b) and (c): Baseline cases. (d), (e) and (f): 16 holes-controlled cases  $\xi = 0.8$ .  
**(Flow from left to right).**

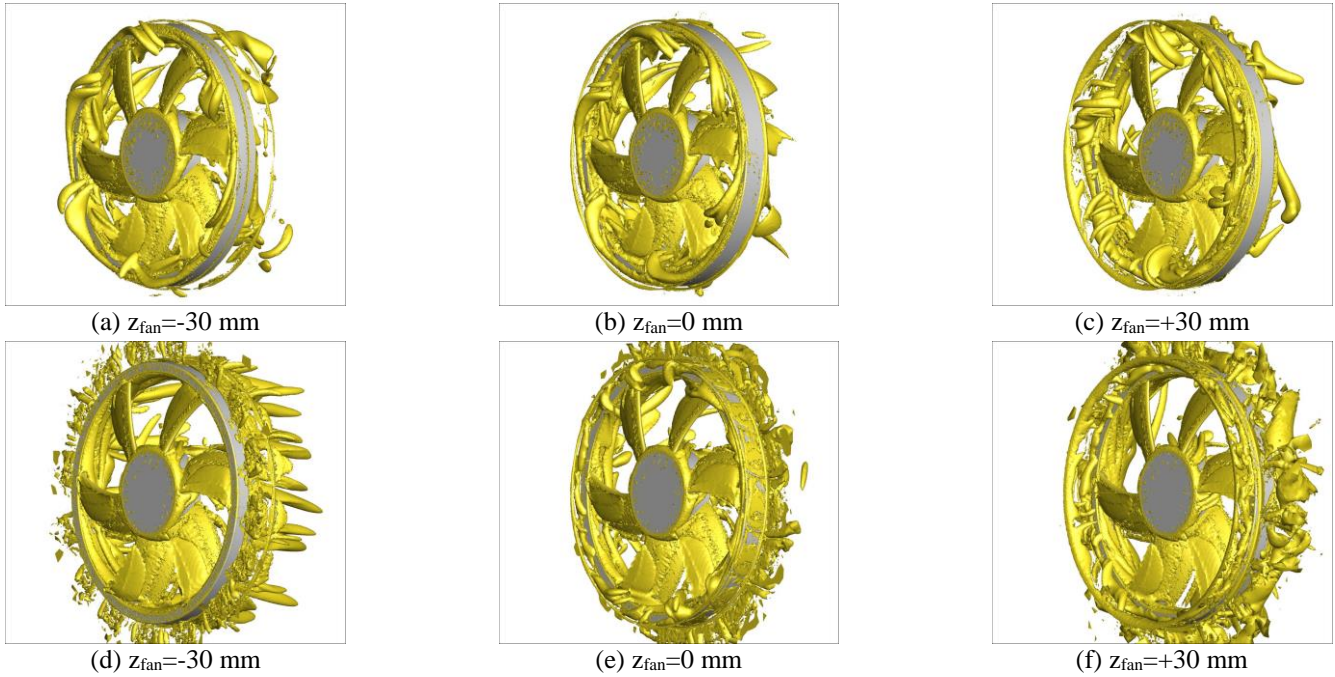


**Fig. 8:** Vorticity analyses using Q criterion for the diaphragm diameter 375 mm, rotating speed 1000 rpm. (a), (b) and (c) : Baseline cases. (d), (e) and (f): 16 holes-controlled cases  $\xi=0.8$ . (Flow from left to right).

#### 4.2. Numerical fan characteristics

The experimental and numerical outcomes in terms of fan aerualic characteristics are shown in figure 9. The numerical simulation predicts almost the same fluctuation tendency of fan characteristics under the injection rate effects, especially for high flow coefficients.

The performance improvement for both controlled and baseline configurations issued from the numerical analysis agree well with each other for the injection rate of  $\xi = 0.8$ . Whereas, for injection rate of  $\xi = 0.4$ , a significant shift between curves is recorded.

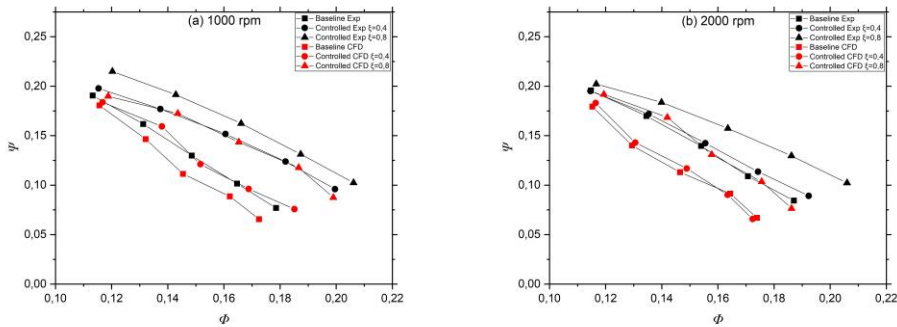


**Fig. 9:** Numerical fan characteristics for 16 holes air injection for  $z_{fan} = 0$  (a) 1000 rpm (b) 2000 rpm.

### 4.3. Quantitative analyses

In order to fully understand the impact of control on the flow around fans, figures 11 and 12 depict the flow topology for two diaphragm diameters 238 and 375 mm, respectively, created in the radial plane positioned at 01 mm from the movable wall, for a radius  $R = 196$  mm (Fig. 10).

For the diaphragm diameter  $\Phi = 238$  mm (Fig.11) in case of the two rotational speeds 1000 and 2000 rpm, the moving wall effect induces a high tangential velocity of the leakage flow. In addition to that, the axial zone affected by the leakage flow, which is separated from the main flow by a separating line, has of a significant dimension of about  $1.5 \times L$  for the rotation speed 1000 rpm compared to  $0.8 \times L$  at high rotational speed of 2000 rpm. This is likely due to the influence of the axial velocity component, which is significant for a low rotational speed of 1000 rpm.

For the diaphragm diameter  $\Phi = 375$  mm (Fig.12). The axial component of the leakage flow is significant than for the case of  $\Phi = 238$  mm. Furthermore, the vortex structure developed from the evolution of the dividing line, undulates as the diaphragm diameter is increased from  $\Phi = 238$  mm to  $\Phi = 375$  mm.

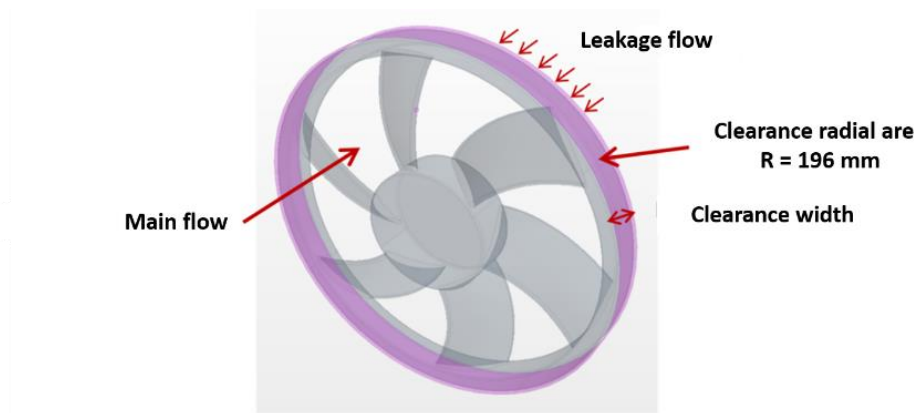


Fig. 10: Radial plane  $R = 196$  mm where results are presented.

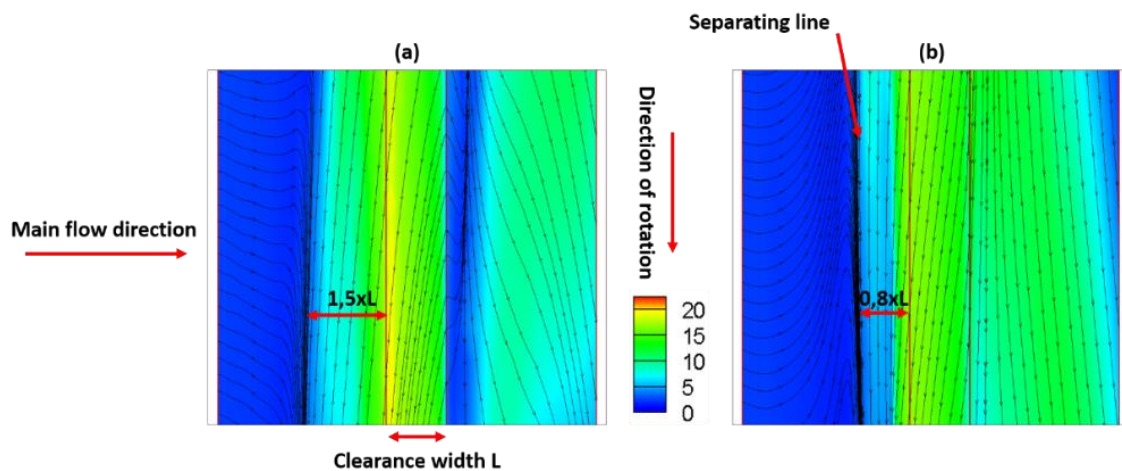
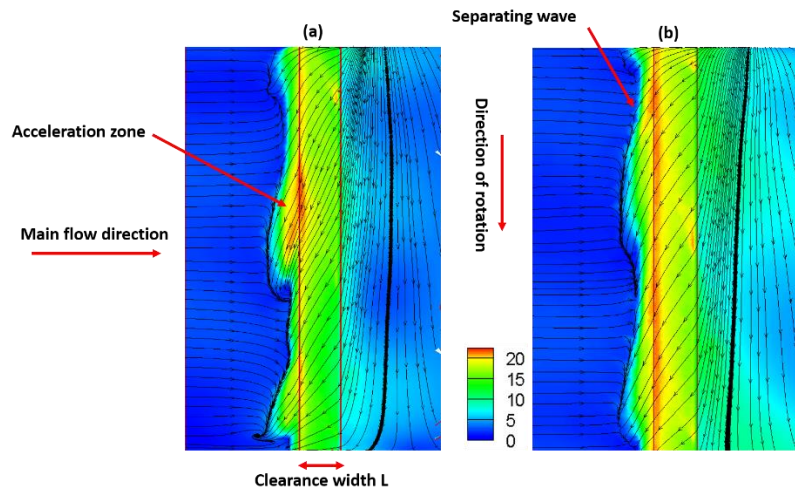


Fig. 11: Absolute velocity in the gap (radius  $R = 196$  mm) for  $\Phi = 238$ . (a) 1000 rpm (b) 2000 rpm.





**Fig. 12:** Absolute velocity in the gap (radius  $R = 196$  mm) for  $\Phi = 375$ . (a) 1000 rpm (b) 2000 rpm.

Figure 14 depicts the static pressure distribution with streamlines in controlled case. Compared to the baseline configuration (Fig. 11 and Fig. 12), complex vortex structures, that are difficult to identify were formed. At the speed of 1000 rpm, the leakage flow was slightly sucked by the effect of the depression generated upstream of the fan. Thus, the results are represented by a reduction in the leakage flow. Between each pair of consecutive holes, a topology similar to that known by “point source” was spotted. Concretely, these source points result from the contact of two recirculation zones in the tangential direction (Fig. 13). In this configuration, the leakage flow remains confined in the gap. At the exit of the gap (upstream), the size of the vortex upstream of the fan becomes larger at the diameter  $\Phi = 238$  mm compared to that of  $\Phi = 375$  mm. It is also clearer that for the controlled case, the swirling zone was remained, as seen in figure 14.

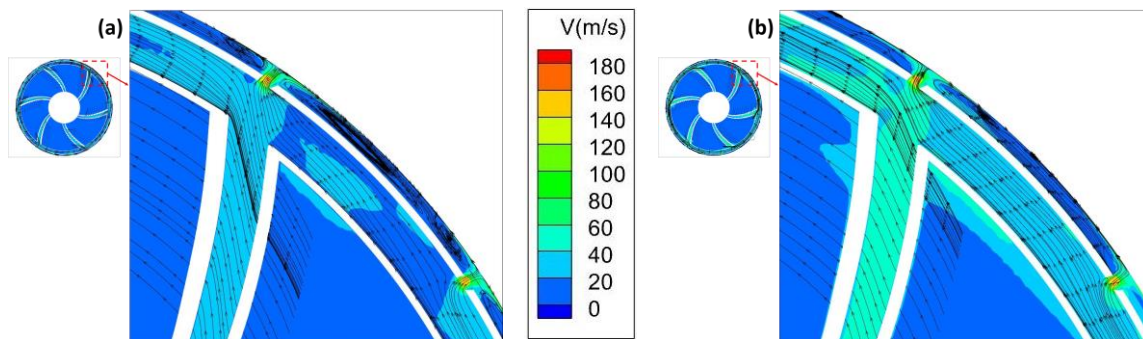


**Fig. 13:** Flow structure for the controlled case near a hole ( $\Phi = 375$  mm,  $\xi = 0.8$ ). (a) 1000 rpm and (b) 2000 rpm.

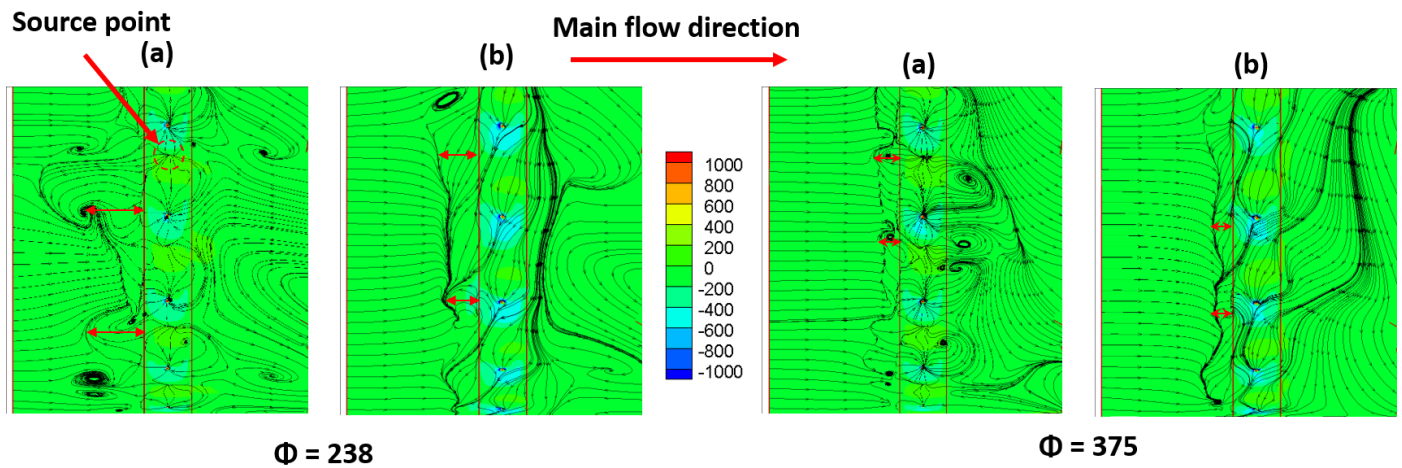


**Fig. 14:** Flow structure of the controlled case ( $\xi = 0.8$ ) in the gap colored by the static pressure distribution. (a) 1000 rpm, (b) 2000 rpm (Left)  $\Phi = 238$  mm, (Right)  $\Phi = 375$  mm

## 5. Conclusion

A rotomolded fan for automotive engine cooling is tested in a casing to simulate its operating conditions (engine cooling), this configuration gives rise to a leakage flow in the gap between the fan and the casing, which is considered as the main source of noise emission and performances reduction. The objective of this study is to actively control this leakage flow by injecting air through 16 holes that have been perforated in the fan shroud ring and are situated and oriented appropriately. Given the significant increase in hydraulic power of roughly 53% and the 80% reduction in leakage flow, it indicates that this approach to control proved to be efficient for this particular configuration.

The swirling zone that forms around the shroud ring due to the interaction between the main flow and the leaking one has a significant impact on the topology of the flow created by the fan. Even when using the control with 16 holes, this swirling zone continues to exist.

Finally, another possibility of injecting momentum to the main flow can be used by replacing the holes with a slot on the whole fan periphery, exhibiting different locations and sizes as depicted in the figure 15.



**Fig. 15:** Proposed injection strategy through Slot.

## References

- [1] C. Sarraf, H. Nouri, F. Ravelet, and F. Bakir, “Experimental study of blade thickness effects on the overall and local performances of a Controlled Vortex Designed axial-flow fan,” *Exp. Therm. Fluid Sci.*, vol. 35, no. 4, pp. 684–693, 2011, doi: 10.1016/j.expthermflusci.2011.01.002.
- [2] J. Hurault, S. Kouidri, F. Bakir, and R. Rey, “Experimental and numerical study of the sweep effect on three-dimensional flow downstream of axial flow fans,” *Flow Meas. Instrum.*, vol. 21, no. 2, pp. 155–165, 2010, doi: 10.1016/j.flowmeasinst.2010.02.003.
- [3] H. B. SQUIRE and K. G. WINTER, “The Secondary Flow in a Cascade of Airfoils in a Nonuniform Stream,” *J. Aeronaut. Sci.*, vol. 18, no. 4, pp. 271–277, 1951, doi: 10.2514/8.1925.
- [4] J. Boudet, A. Cahuzac, P. Kausche, and M. C. Jacob, “Zonal large-eddy simulation of a fan tip-clearance flow, with evidence of vortex wandering,” *J. Turbomach.*, vol. 137, no. 6, pp. 1–9, 2015, doi: 10.1115/1.4028668.
- [5] T. Zhu and T. H. Carolus, “Experimental and numerical investigation of the tip clearance noise of an axial fan,” *Proc. ASME Turbo Expo*, vol. 4, no. April 2014, 2013, doi: 10.1115/GT2013-94100.
- [6] D. You, M. Wang, P. Moin, and R. Mittal, “Effects of tip-gap size on the tip-leakage flow in a turbomachinery cascade,” *Phys. Fluids*, vol. 18, no. 10, 2006, doi: 10.1063/1.2354544.
- [7] E. Canepa, A. Cattanei, F. Mazzocut Zecchin, and D. Parodi, “Large-scale unsteady flow structures in the leakage flow of a low-speed axial fan with rotating shroud,” *Exp. Therm. Fluid Sci.*, vol. 102, no. June 2018, pp. 1–19, 2019, doi: 10.1016/j.expthermflusci.2018.10.020.
- [8] T. Azzam, R. Paridaens, F. Ravelet, S. Khelladi, H. Oualli, and F. Bakir, “Experimental investigation of an actively controlled automotive cooling fan using steady air injection in the leakage gap,” *Proc. Inst. Mech. Eng. Part A J. Power Energy*, vol. 231, no. 1, pp. 59–67, 2017, doi: 10.1177/0957650916688120.
- [9] M. Pereira *et al.*, “Improved aerodynamics of a hollow-blade axial flow fan by controlling the leakage flow rate by air injection at the rotating shroud,” *Entropy*, vol. 23, no. 7, 2021, doi: 10.3390/e23070877.
- [10] M. Eberlinc, B. Širok, and M. Hočevár, “Experimental investigation of the interaction of two flows on the axial fan hollow blades by flow visualization and hot-wire anemometry,” *Exp. Therm. Fluid Sci.*, vol. 33, no. 5, pp. 929–937, 2009, doi: 10.1016/j.expthermflusci.2009.03.012.
- [11] K. Park, H. Choi, S. Choi, and Y. Sa, “Effect of a casing fence on the tip-leakage flow of an axial flow fan,” *Int. J. Heat Fluid Flow*, vol. 77, no. June 2018, pp. 157–170, 2019, doi: 10.1016/j.ijheatfluidflow.2019.04.005.
- [12] F. Wasilczuk, P. Flaszynski, P. Kaczynski, R. Szwaba, P. Doerffer, and K. Marugi, “Air curtain application for leakage reduction in gas turbine shroud sealing,” *Aerosp. Sci. Technol.*, vol. 112, p. 106636, 2021, doi: 10.1016/j.ast.2021.106636.
- [13] International Organization for Standardization, “« Ventilateurs industriels - Essais aérauliques sur circuits normalisés (ISO 5801) ».” 2007.